

AD-A091 802

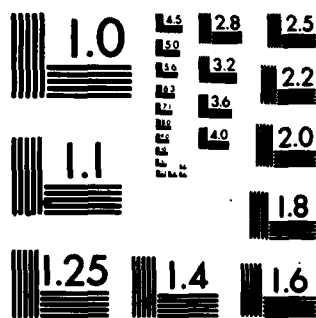
NAVAL RESEARCH LAB WASHINGTON DC  
LONG TERM VARIABILITY OF WINDSPEED.(U)  
NOV 80 A I ELLER, M L BLODGETT

F/6 4/2

UNCLASSIFIED NRL-8436

NI

END  
DATE  
FILMED  
1-8  
DTIC



MICROCOPY RESOLUTION TEST CHART  
NATIONAL BUREAU OF STANDARDS-1963-A

AD A091802

SECRET

SECURITY CLASSIFICATION OF THIS PAGE (When Data Entered)

REPORT DOCUMENTATION PAGE		READ INSTRUCTIONS BEFORE COMPLETING FORM
1. REPORT NUMBER <b>NRL Report 8436</b>	2. GOVT ACCESSION NO. <b>AD-A091802</b>	3. RECIPIENT'S CATALOG NUMBER
4. TITLE (and Subtitle) <b>LONG TERM VARIABILITY OF WINDSPEED</b>		5. TYPE OF REPORT & PERIOD COVERED <b>An interim report on a continuing NRL problem.</b>
7. AUTHOR(s) <b>A. I. Eller and M. L. Blodgett</b>		6. PERFORMING ORG. REPORT NUMBER
8. PERFORMING ORGANIZATION NAME AND ADDRESS <b>Naval Research Laboratory Washington, DC 20375</b>		9. CONTRACT OR GRANT NUMBER(s) <b>14R0120SH</b>
11. CONTROLLING OFFICE NAME AND ADDRESS <b>Naval Ocean Research &amp; Development Activity NSTL Station, MS 39529</b>		10. PROGRAM ELEMENT, PROJECT, TASK AREA & WORK UNIT NUMBERS <b>63795N R0120SH 81-0353-0-0</b>
14. MONITORING AGENCY NAME & ADDRESS (if different from Controlling Office)		12. REPORT DATE <b>November 1988</b>
		13. NUMBER OF PAGES <b>24</b>
		15. SECURITY CLASS. (of this report) <b>UNCLASSIFIED</b>
		15a. DECLASSIFICATION/DOWNGRADING SCHEDULE
16. DISTRIBUTION STATEMENT (of this Report)  <b>Approved for public release; distribution unlimited.</b>		
17. DISTRIBUTION STATEMENT (of the abstract entered in Block 20, if different from Report)		
18. SUPPLEMENTARY NOTES  <b>*A. I. Eller is now with Science Applications Inc., McLean, VA</b>		
19. KEY WORDS (Continue on reverse side if necessary and identify by block number)  <b>Wind speed, synoptic variability</b>		
20. ABSTRACT (Continue on reverse side if necessary and identify by block number) <b>Underwater acoustic sensors are subject to interfering ambient noise generated by the action of wind on the sea surface. Noise at frequencies above a few hundred Hz generally shows strong correlation with wind speed. A knowledge of the statistical variability of wind-speed is useful for predicting the properties of ambient noise. Values of surface wind speed and atmospheric pressure reported from weather stations at Jan Mayen in the Norwegian Sea and Bear Island in the Barents Sea over a two-year period were examined. It was found that the statistical distribution of wind speeds can be represented approximately as a Rayleigh distribution. Spectral analysis of the time series records of wind speed and</b> (Continues)		

DD FORM 1473  
1 JAN 73

EDITION OF 1 NOV 68 IS OBSOLETE  
S/N 0102-014-8601

SECURITY CLASSIFICATION OF THIS PAGE (When Data Entered)

20100

JCE

20. Abstract (Continued)

pressure shows that most of the variability of these parameters is contributed by synoptic scale variations having periods of from a few days to a few weeks. The annual or seasonal variation has the largest single Fourier coefficient but represents only a relatively small part of the total variance.

## CONTENTS

INTRODUCTION .....	1
WIND SPEED VARIABILITY AND STATISTICS .....	1
PROBABILITY DENSITY AND CUMULATIVE DISTRIBUTION FUNCTIONS .....	5
FLUCTUATION SPECTRA .....	10
DISCUSSION AND SUMMARY .....	17
REFERENCES .....	17
APPENDIX — Fourier Analysis of Wind Speed Data .....	19

Account for	
NIS GRA&I	<input checked="checked" type="checkbox"/>
DTIC TAB	<input type="checkbox"/>
Unannounced	<input type="checkbox"/>
Justification	
By _____	
Distribution/	
Availability Codes	
Dist	Avail and/or Special
A	

## LONG TERM VARIABILITY OF WINDSPEED

### INTRODUCTION

Measurements of ambient ocean acoustic noise at frequencies from a few hundred hertz to several kilohertz generally show strong correlation with wind speed. Ambient noise is correlated with surface wave height, also, but to a lesser degree, and thus wind speed appears to be the single most important weather variable needed in making predictions of ambient noise. In support of the need of the environmental acoustics community to be able to predict ambient noise variability, this report describes the statistical variability and fluctuation spectrum of long term records of wind speed, obtained from two weather stations. A brief review is given also of results from previous studies of wind speed fluctuations. The present results are used in part to extend the frequency range of previously reported wind speed fluctuation spectra. Time scales of interest here are those corresponding to synoptic variability, which has periods of days to months, and to seasonal or yearly variation. Brief attention is paid also to records of sea level atmospheric pressure. This variable shows correlation with wind speed and may be of some use in noise prediction.

The data that form the basis of this report include values of surface wind speed recorded every 12 h over the 2-yr interval from 1 June 1974 to 31 May 1976 at Bear Island (World Meteorological Organization, WMO, Station 1028, 74°N, 19°E) and at Jan Mayen (WMO Station 1001, 71°N, 8°W). Bear Island is located in the Barents Sea, and Jan Mayen, in the Norwegian Sea. A second and smaller data set, consisting of wind speed values every 3 h from 1 July 1974 to 31 January 1975 at Bear Island, was also available and was used to extend the high-frequency end of the fluctuation spectrum. These two stations were chosen in order that the results could add to other Naval Research Laboratory studies of this area.

### WIND SPEED VARIABILITY AND STATISTICS

Time series records of surface wind speed and atmospheric pressure are displayed in Figs. 1 through 4. Each plot is based on values recorded every 12 h, at noon and midnight, for 2 yr. The data are smoothed with a uniform, rectangular window, giving a 3-day (6-data-point) average. Visual comparison of plots with and without smoothing indicated that the smoothed curves are better able to reveal the variability and trends over the time periods of interest. Each curve shows an annual seasonal variability, with wind speed generally greater in winter than in summer and atmospheric pressures generally greater in summer. It is also apparent in these figures that variability over shorter time periods, from a few days to a month, is greater than the seasonal variability.

Monthly statistics of wind speed at each station are summarized in Table 1. The first column for each station gives the number of samples available each month. This number

ELLER AND BLODGETT

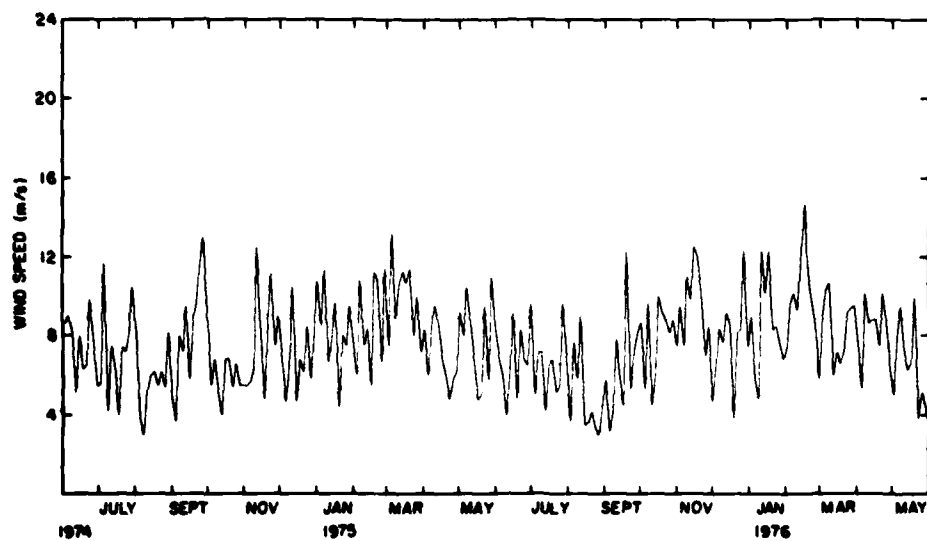


Fig. 1 - Smoothed time series record of wind speed at Bear Island, June 1974 through May 1976

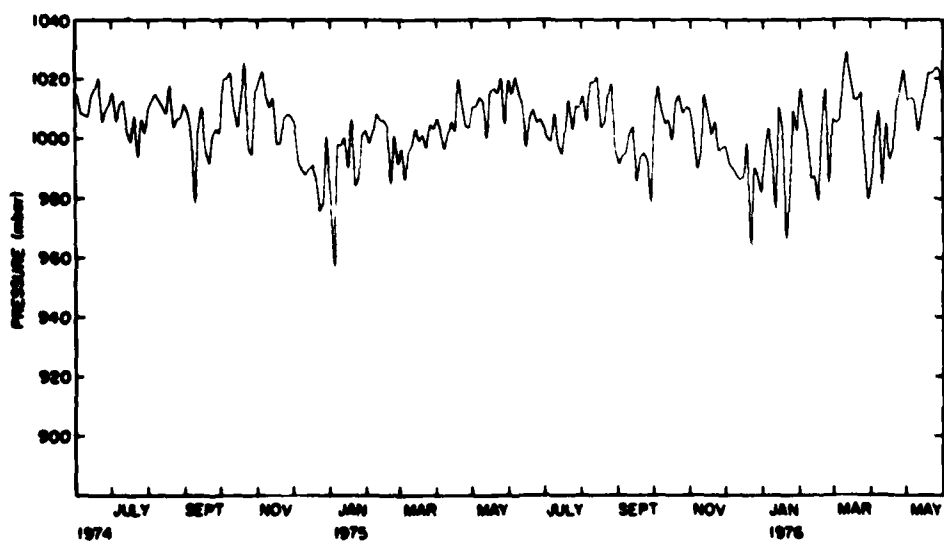


Fig. 2 - Smoothed time series record of atmospheric pressure at Bear Island, June 1974 through May 1976



NRL REPORT 8436

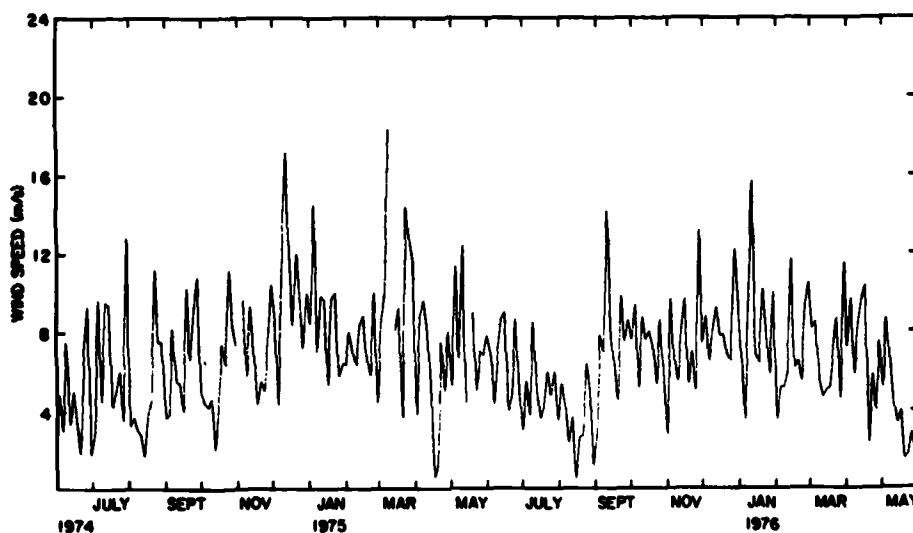


Fig. 3 — Smoothed time series record of wind speed at Jan Mayen, June 1974 through May 1976

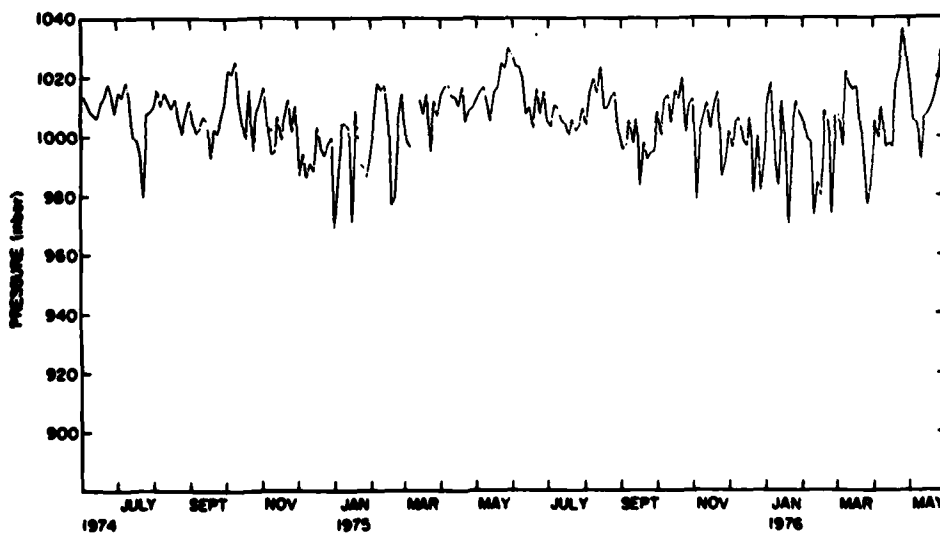


Fig. 4 — Smoothed time series record of atmospheric pressure at Jan Mayen, June 1974 through May 1976.

ELLER AND BLODGETT

Table 1 — Monthly Statistics of Windspeed

Time	Station 1001					Station 1028				
	# Samples	Avg m/s	$\sigma$ m/s	Skewness	Kurtosis	# Samples	Avg m/s	$\sigma$ m/s	Skewness	Kurtosis
1974										
June	48	4.8	3.3	0.20	-0.34	57	7.4	2.6	-0.06	-0.47
July	42	7.3	4.4	0.31	-0.36	56	7.3	3.8	0.22	-0.46
Aug.	49	5.0	4.0	0.65	0.62	54	5.8	3.3	0.70	2.09
Sept.	47	6.8	3.6	0.17	-0.42	55	8.4	4.1	0.24	-0.26
Oct.	46	6.4	3.9	0.59	1.34	57	6.0	2.3	0.15	-0.01
Nov.	39	7.4	3.4	0.35	-0.08	57	7.9	3.7	0.50	0.49
Dec.	55	10.3	4.4	0.14	-0.32	60	7.1	3.3	0.30	0.01
1975										
Jan.	48	8.9	4.3	0.07	-0.49	58	8.2	4.0	0.05	-0.41
Feb.	47	7.6	3.8	-0.25	-0.12	54	8.6	3.8	0.09	0.00
Mar.	38	10.4	5.2	-0.02	-0.57	57	9.6	4.0	0.31	0.22
Apr.	43	5.9	3.8	0.01	-0.54	55	7.1	2.9	0.32	-0.08
May	35	7.6	3.9	0.20	-0.27	58	7.9	3.4	0.14	-0.03
June	43	6.5	3.6	0.20	-0.47	55	6.9	2.4	0.03	-0.28
July	31	4.8	2.2	0.13	0.28	58	6.6	2.9	0.05	-0.15
Aug.	48	3.5	2.8	0.20	-0.44	60	4.9	2.8	0.37	0.58
Sept.	47	7.6	4.8	0.03	-0.48	57	6.5	4.0	0.32	-0.16
Oct.	54	6.9	4.2	0.24	0.04	59	7.7	4.2	0.22	-0.11
Nov.	52	7.7	3.8	0.33	-0.09	55	9.3	4.0	0.13	-0.23
Dec.	55	8.1	3.8	0.42	0.33	59	8.1	4.3	0.61	0.69
1976										
Jan.	61	8.4	4.7	0.23	-0.08	62	8.4	4.1	0.20	-0.38
Feb.	56	6.6	3.5	0.35	0.01	56	9.9	4.1	0.35	0.08
Mar.	58	7.2	3.8	0.50	0.67	58	8.7	3.4	0.12	-0.18
Apr.	59	7.1	4.0	0.20	0.45	60	8.0	3.6	0.13	-0.32
May	62	4.2	3.9	0.55	0.52	62	6.4	3.2	0.11	-0.35
Overall	1163	7.0	4.3	0.28	-0.01	1379	7.6	3.8	0.31	0.16

# NRL REPORT 8436

varies partly because some wind speed values are missing. Values of standard deviation, skewness and kurtosis in the table are based on the following definitions [1]:

$$\text{Standard deviation} = \left[ \frac{\sum_i (x_i - \bar{X})^2}{N} \right]^{1/2} \quad (1)$$

$$\text{Skewness} = \frac{\sum_i (x_i - \bar{X})^3}{2N\sigma^3} \quad (2)$$

$$\text{Kurtosis} = \frac{\sum_i (x_i - \bar{X})^4}{2N\sigma^4} - \frac{3}{2} \quad (3)$$

Monthly values of standard deviation show moderate correlation (correlation of 0.70 at Jan Mayen and 0.65 at Bear Island) with monthly average wind speeds,  $\sigma$  tending to be higher when the average wind speed is higher. Values of skewness and kurtosis show relatively large fluctuations from month to month.

## PROBABILITY DENSITY AND CUMULATIVE DISTRIBUTION FUNCTIONS

Probability density functions and cumulative distributions of wind speed were computed for each station and are shown in Figs. 5 through 8. The appearance of the probability density functions is similar to that of the Rayleigh distribution

$$f(u) = \frac{u}{S^2} \exp \left( -\frac{1}{2} \frac{u^2}{S^2} \right), \quad (4)$$

where  $u$  is the wind speed and  $S$  is an adjustable parameter. The cumulative distributions give the percentage of wind speeds less than the abscissa and are plotted on probability paper. A cumulative Rayleigh distribution, given by  $1 - \exp(-u^2/2S^2)$ , was fitted to the data of each station, and the corresponding curves are indicated in Figs. 6 and 8. The value of the parameter  $S$  for Station 1028 was chosen such that the median wind speed is the same for the fitted curve and the data. This value is  $S = 5.65$ , determined from the relation

$$S = \frac{\text{median wind speed}}{(2 \ln 2)^{1/2}} \quad (5)$$

ELLER AND BLODGETT

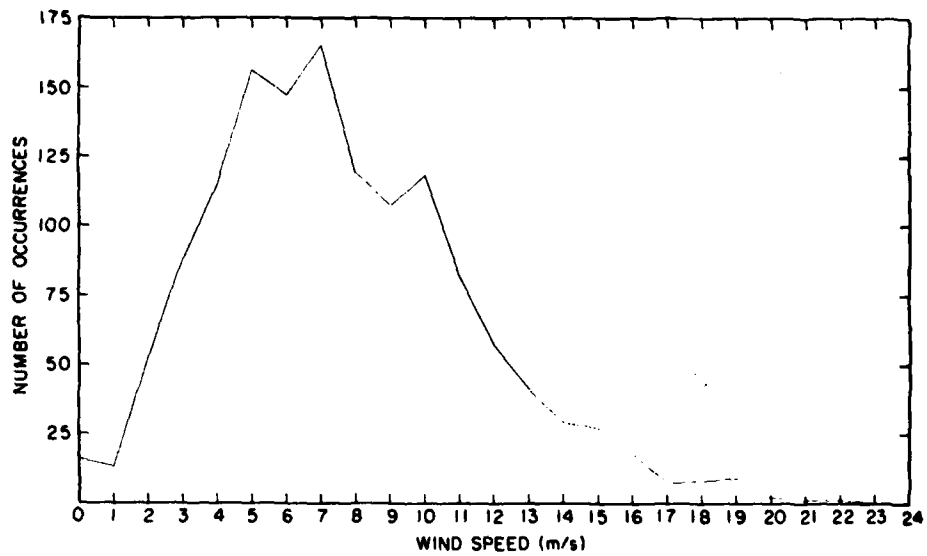


Fig. 5 — Probability density function of wind speed at Bear Island,  
June 1974 through May 1976

NRL REPORT 8436

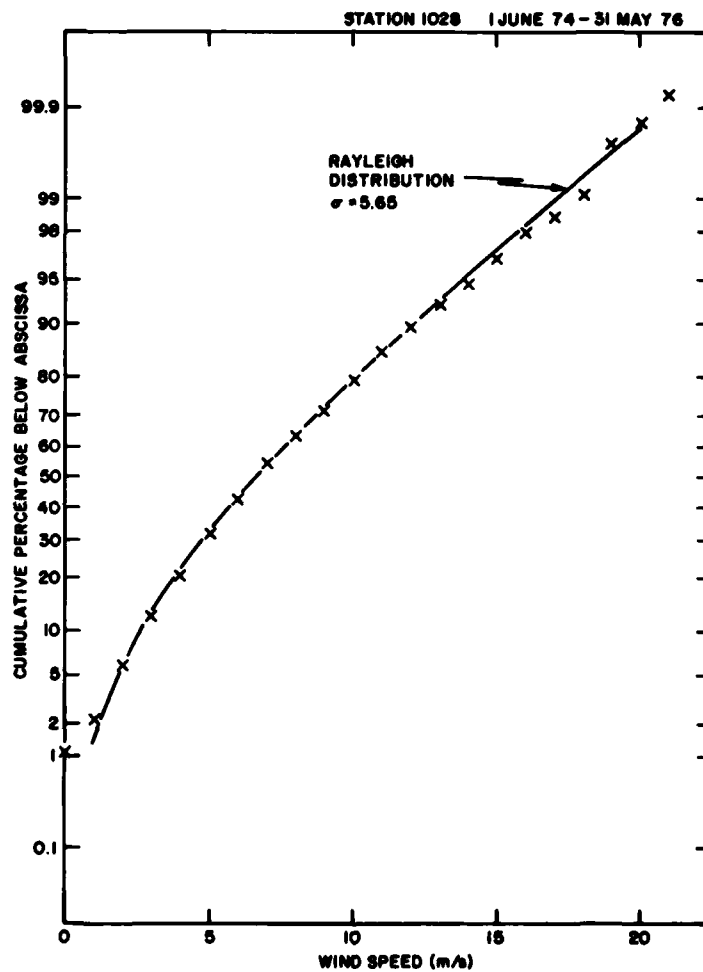


Fig. 6 — Cumulative distribution of wind speeds at Bear Island, June 1974 through May 1976. Curve corresponds to Rayleigh distribution with  $S = 5.65$ .

ELLER AND BLODGETT

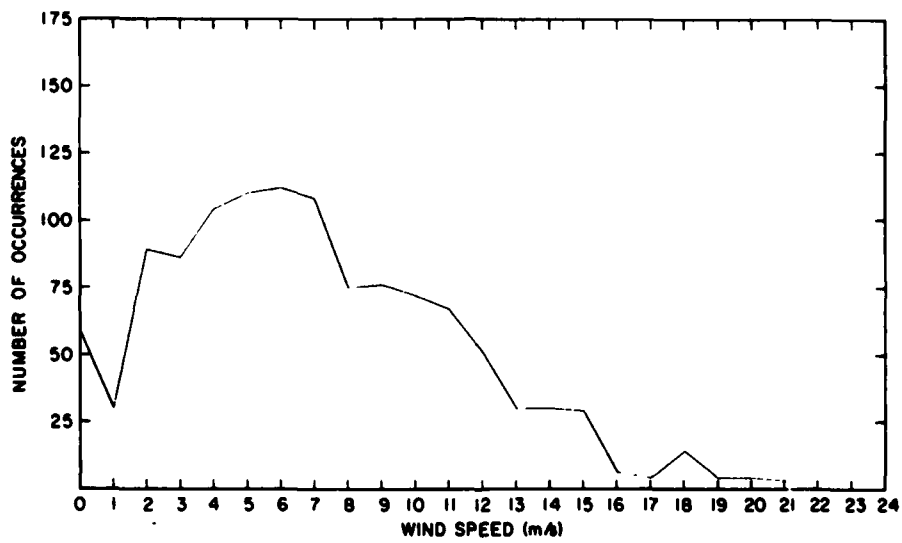


Fig. 7 — Probability density function of wind speed at Jan Mayen, June 1974 through May 1976

NRL REPORT 8436

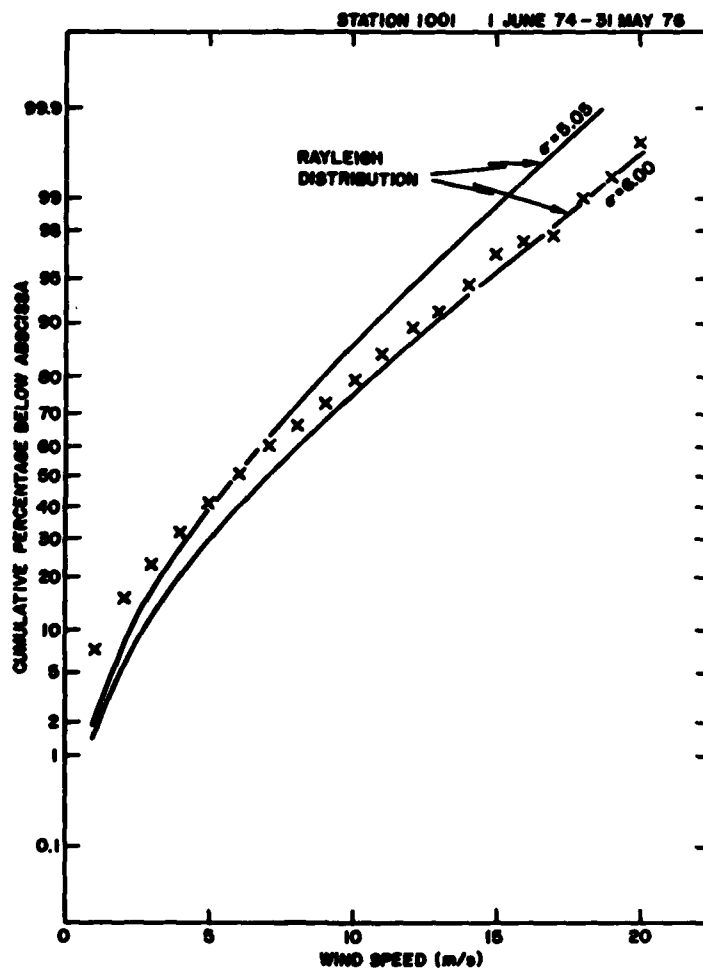


Fig. 8 — Cumulative distribution of wind speeds at Jan Mayen, June 1974 through May 1976. Curves correspond to Rayleigh distribution with  $S = 5.05$  and  $S = 6.00$ .

The resulting computed curve agrees well with the data, shown by the symbols. A similar approach for Station 1001 gives  $S = 5.05$ ; the resulting computed curve shows poorer agreement than was found at the other station. The cumulative Rayleigh distribution for  $S = 6.00$  is illustrated, also, for the purpose of comparison.

Other tests that can be used to measure the closeness of the data to a Rayleigh distribution are to compare values of the coefficient of variation (defined as the standard deviation divided by the average), the skewness, and the kurtosis. Calculated values of these quantities for a Rayleigh distribution are compared to the measured values at each Station in Table 2. It is noted that the calculated values for a Rayleigh distribution are independent of the parameter  $S$ .

It is concluded from Table 2 as well as from Figs. 5 through 8 that as an approximation the distribution of wind speeds can be modeled as a Rayleigh distribution. This model produces a better fit to the data at Bear Island than at Jan Mayen.

### FLUCTUATION SPECTRA

The time series of wind speed and atmospheric pressure values at each station were analyzed into frequency components by means of a discrete Fourier transform. The resulting frequency components were then used to form the wind speed and pressure fluctuation spectra, which are presented in Figs. 9 through 13. Figures 11 through 13 are based on a 2-yr record, data taken every 12 h, for a total of 1462 samples of each variable. Each series gives an upper spectral frequency of  $1/24$  cph. Figure 10 is based on a 6-month record from July through December 1974, with values every 3 h. The higher sample rate results in an upper spectral frequency of  $1/6$  cph. The spectrum in Fig. 9 is combined from both the 2-yr and the 6-month records and has the broadest spectral range available from the data. The two spectral portions are joined at a frequency of approximately 0.026 cph, the lower-frequency portion coming from the 2-yr record, and the higher-frequency portion from the 6-month record. The wind fluctuation spectra in Figs. 9, 10 and 12 have been smoothed with a sliding 1-3-5-3-1 frequency window.

The largest single frequency component of each variable is the annual component. For wind speed, the peak amplitude annual components at Bear Island and Jan Mayen are 1.3 m/s and 1.7 m/s, respectively. (Note that the ordinates in Figs. 9 through 13 give the spectral density, which is the mean square of the Fourier frequency component divided by

Table 2. — Comparison of Measured and Rayleigh Values of Coefficient of Variation, Skewness, and Kurtosis

	Rayleigh	Sta. 1001 Jan Mayen	Sta. 1028 Bear Island
coeff. of var.	0.52	0.62	0.49
skewness	0.32	0.28	0.31
kurtosis	0.12	-0.01	0.16



NRL REPORT 8436

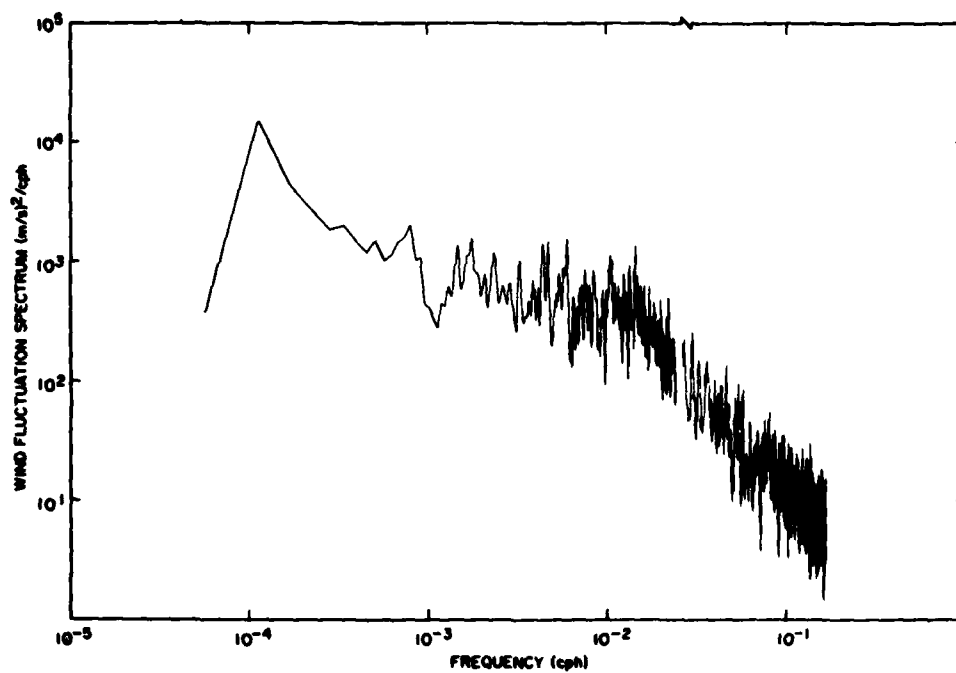


Fig. 9 - Wind fluctuation spectrum based on 2-yr and 6-month data records at Bear Island, June 1974 through May 1976

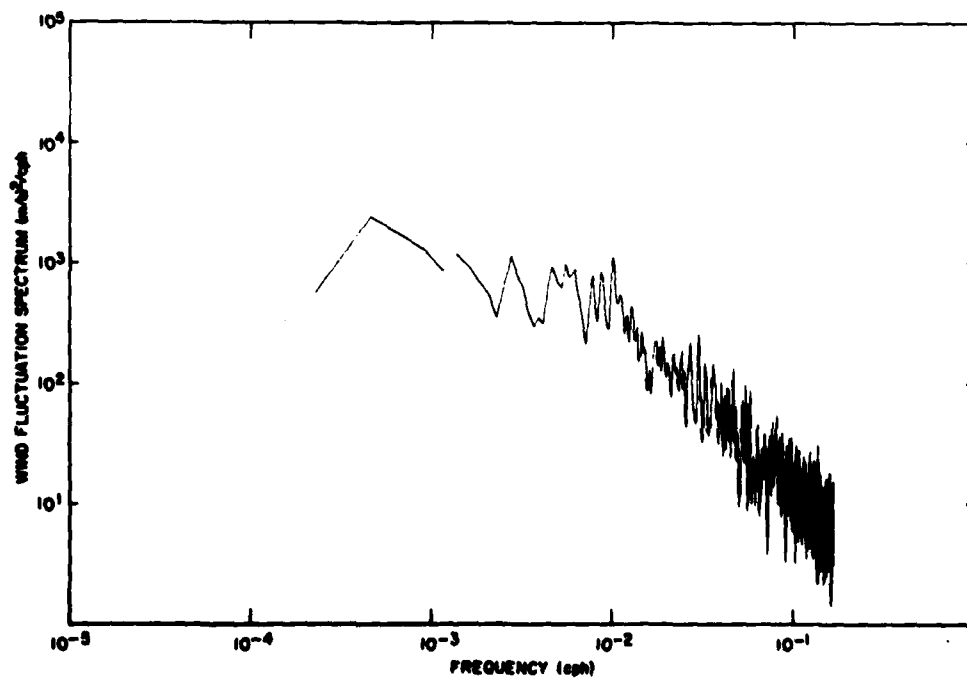


Fig. 10 - Wind fluctuation spectrum at Bear Island, July 1 through December 1974

ELLER AND BLODGETT

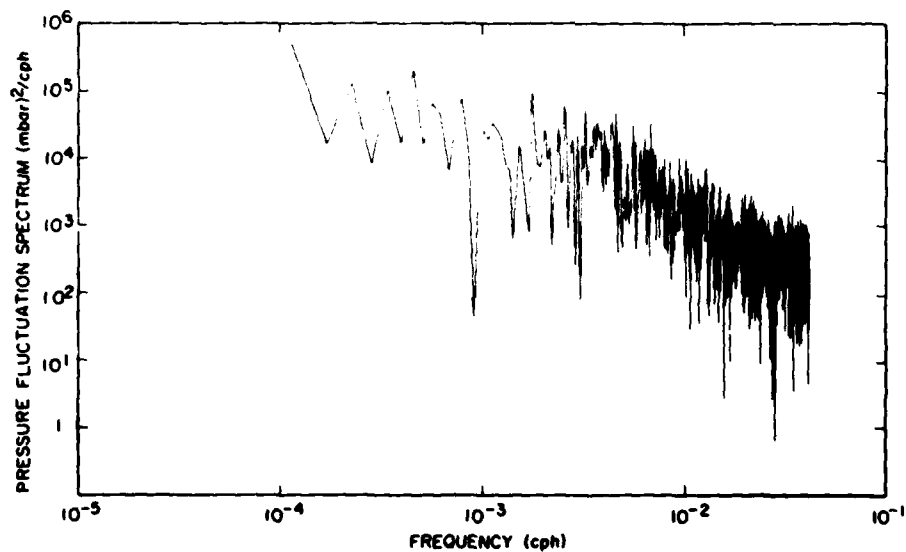


Fig. 11 — Pressure fluctuation spectrum at Bear Island, June 1974 through May 1976

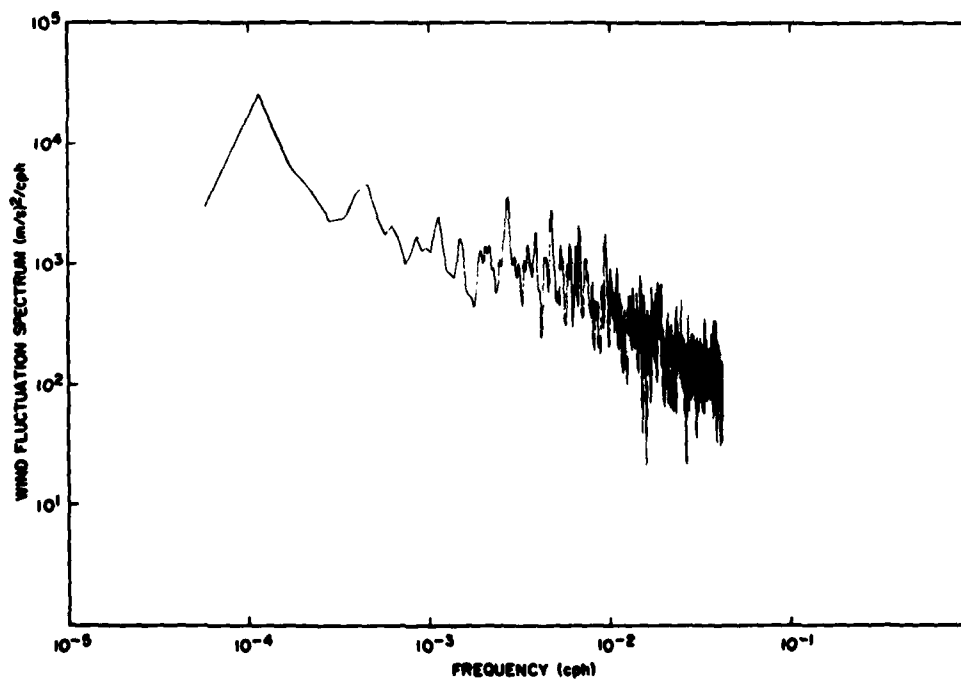


Fig. 12 — Wind fluctuation spectrum at Jan Mayen, June 1974 through May 1976

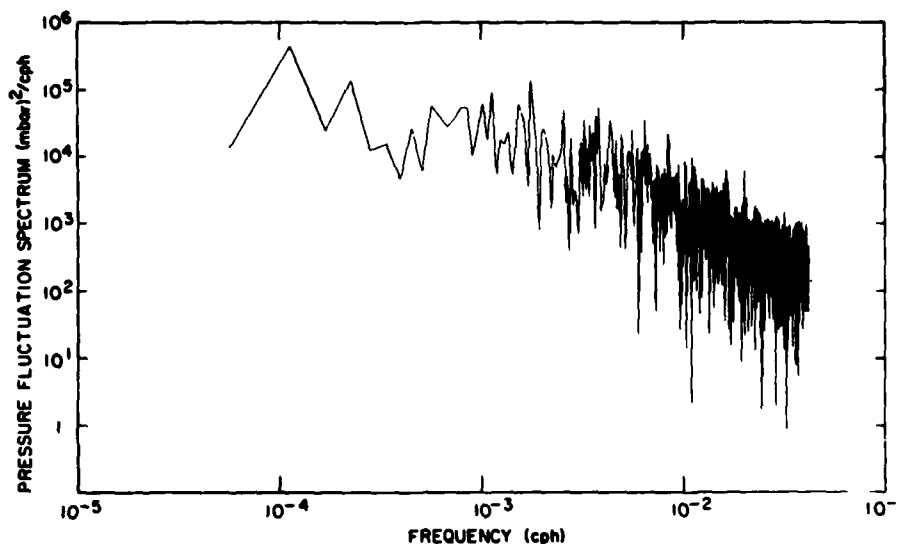


Fig. 13 — Pressure fluctuation spectrum at Jan Mayen, June 1974 through May 1976

the fundamental frequency.) These annual components are relatively small as compared to the total variability of wind speed values. The variance associated with the annual wind speed component is  $0.88 \text{ (m/s)}^2$  at Bear Island and  $1.44 \text{ (m/s)}^2$  at Jan Mayen, in each case much less than the corresponding total variances of  $14.1 \text{ (m/s)}^2$  and  $18.3 \text{ (m/s)}^2$ , respectively. Thus, seasonal variability constitutes a relatively small portion (approximately 7 percent) of the total variance of wind speed at each station. The question of where in the spectrum most of the variability is found is considered later. Peak amplitude annual components of atmospheric pressure are 760 Pa (7.6 mbar) and 700 Pa (7.0 mbar) at Bear Island and Jan Mayen.

At high frequencies, the wind fluctuation spectrum decreases at a rate that appears slightly greater than  $f^{-1}$ ; at lower frequencies the slope is much less. Transition from low to high fluctuation frequency for the wind speed appears to fall in the spectral band near  $10^{-2}$  cph, corresponding to a period of about 4 days. The 6-month spectrum of Fig. 10 shows a moderate peak at  $10^{-2}$  cph. The pressure fluctuation spectra have a high frequency slope of about  $f^{-3/2}$ , with a transition to the high-frequency asymptote at approximately 0.003 cph, corresponding to a period of about 2 weeks.

Figures 14 through 18 present a quantity that has become known [2] as the logarithmic spectrum, each corresponding respectively to the spectra in Figs. 9 through 13. The ordinate represents the product of the fluctuation spectrum times the fluctuation frequency, plotted against the logarithm of frequency. An advantage of the logarithmic spectrum is that the variance for any portion of the spectrum is proportional to the area under the curve, while preserving the advantages of using a logarithmic frequency axis. Use of the logarithmic spectrum aids in the recognition of major spectral contributions in proportional frequency bands, rather than in bands of fixed bandwidth. The logarithmic spectra in Figs. 14 through 18 are computed from fluctuation spectra that were first smoothed by a triangular sliding

ELLER AND BLODGETT

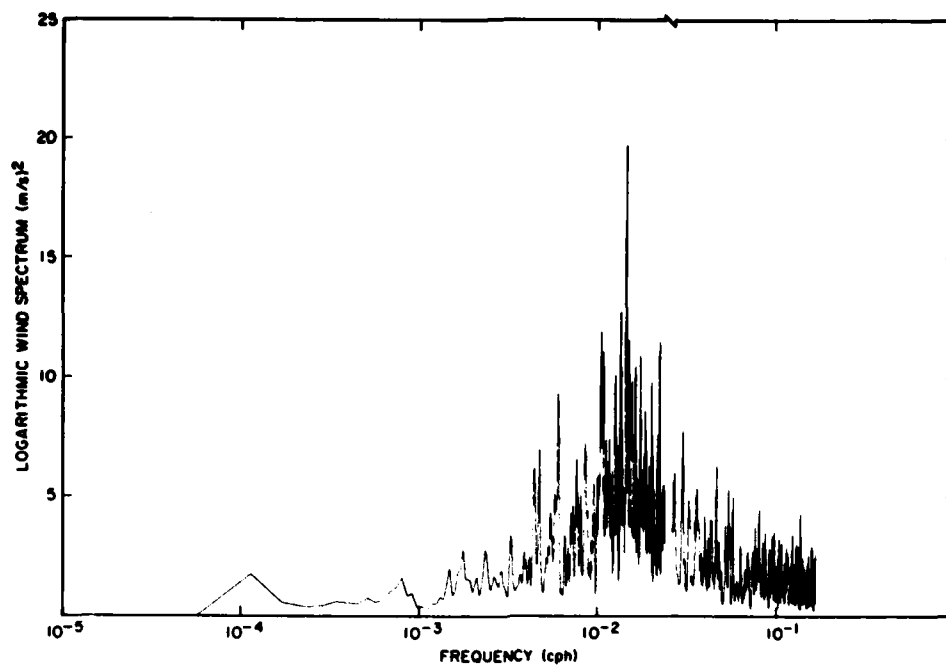


Fig. 14 — Logarithmic wind spectrum based on 2-yr and 6-month data records at Bear Island, June 1974 through May 1976

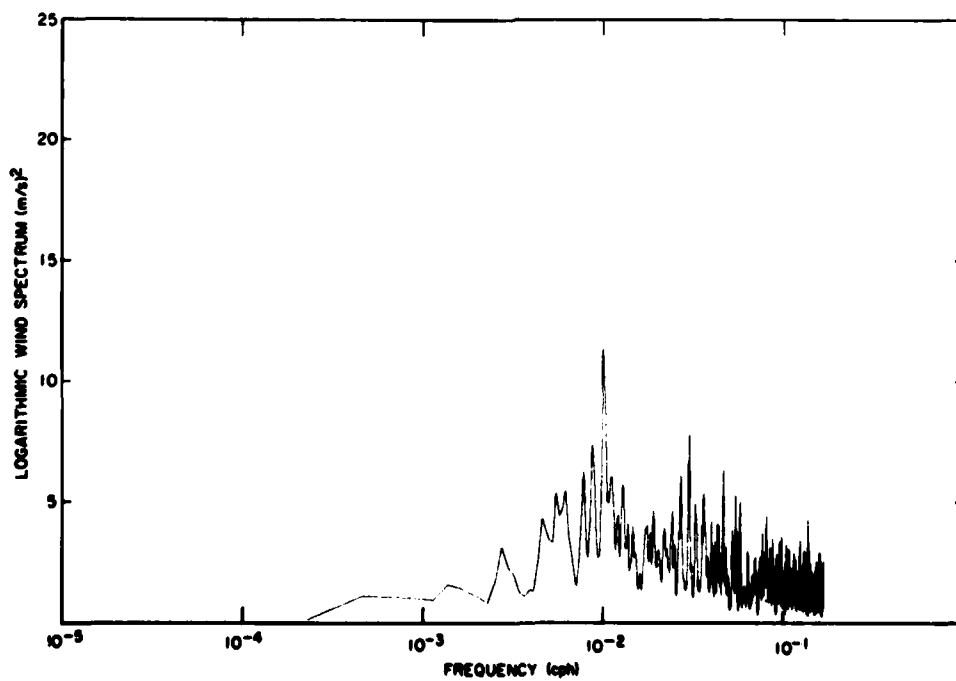


Fig. 15 — Logarithmic wind spectrum at Bear Island, July 1, through December 1974

NRL REPORT 8436

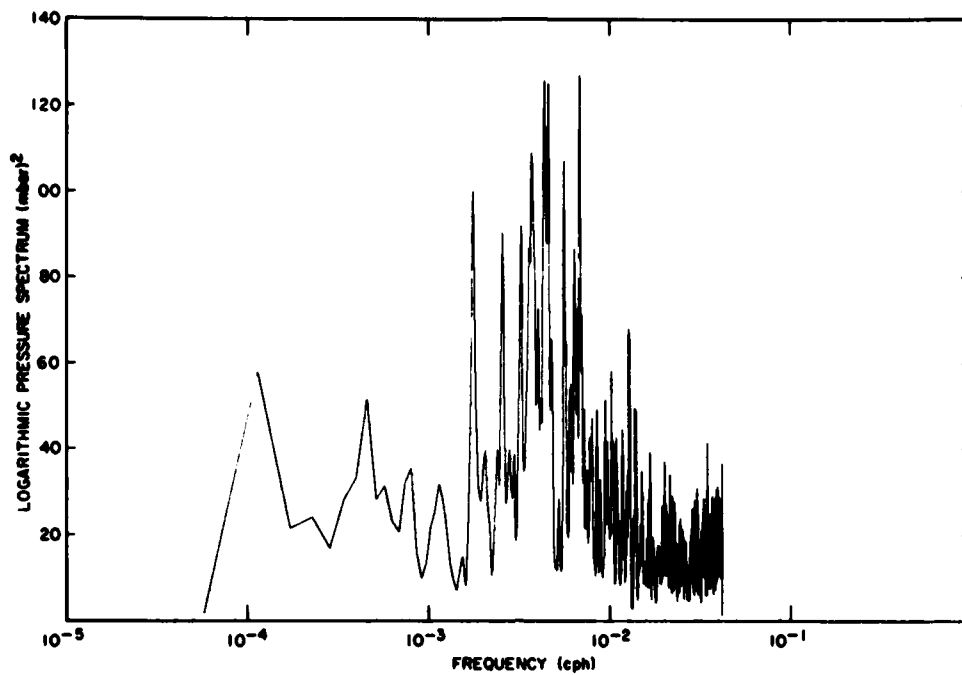


Fig. 16 — Logarithmic pressure spectrum at Bear Island, June 1974 through May 1976

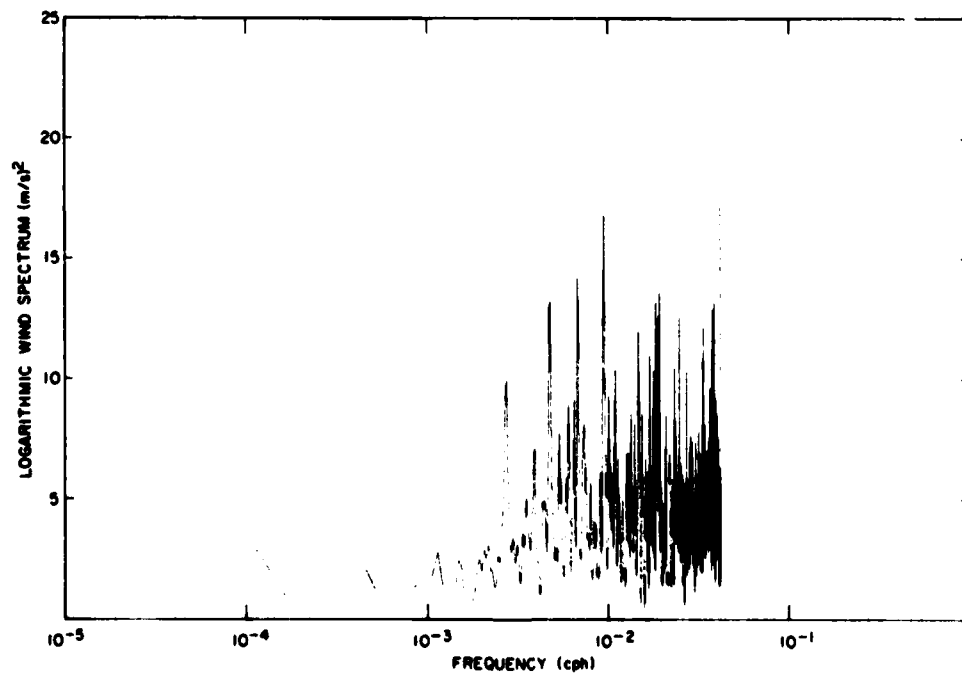


Fig. 17 — Logarithmic wind spectrum at Jan Mayen, June 1974 through May 1976

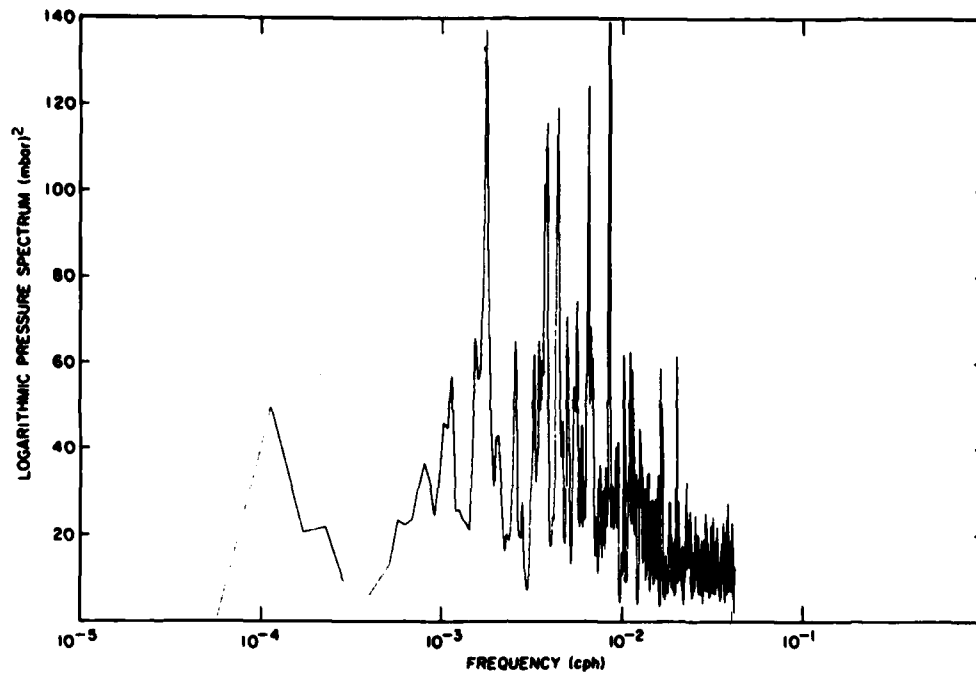


Fig. 18 — Logarithmic pressure spectrum at Jan Mayen, June 1974 through May 1976

frequency window, averaging over five successive values with relative weightings in the ratio 1-3-5-3-1. Figure 14 presents combined results based on the 2-yr as well as the 6-month data records in the same manner as Fig. 9. The logarithmic wind spectra show that most of the variability exists in a broad spectral region whose roughly defined limits correspond to periods of from 2 to 10 days. Figure 15 shows a peak at 0.01 cph, based on the 6-month record, but this peak is not apparent in the 2-yr records. The pressure records show, similarly, that most of the spectral energy exists in a broad spectral band whose roughly defined limits correspond to periods of from 5 to 20 days.

In performing the Fourier analysis of the 2-yr time series of values of wind speed or pressure, it was regarded as necessary to use the entire 2-yr sequence of 1462 values, in order that the annual variation coincide with a harmonic (the second) of the fundamental analysis frequency. Thus, use of the available, conventional FFT algorithm was not possible because, based on a time length other than the full 2-yr, it would tend to smear out the annual spectral contribution. In order to replace the FFT while keeping computation time small, a separate discrete Fourier transform subroutine was written, based on a conventional approach but exploiting the high speed vectorizing capability of the TI-ASC computer. The subroutine can be adapted to any number of data points and is presented in the Appendix.

## DISCUSSION AND SUMMARY

The results of several early studies of wind speed fluctuations are summarized by Van der Hoven [3] in a report that covers an extraordinarily broad spectral range. His aim was to cover a sufficiently broad part of the spectrum "so as to include all important contributions to the total variance." Van der Hoven identifies two major spectral peaks, one centered at a period of 4 days (with a spread from about 2 to 7 days) attributed to the passage of synoptic scale weather patterns, the other at a period of about 1 min and related to the micrometeorological turbulence. The reported peak at 4 days has a logarithmic spectral level of about  $5 \text{ (m/s)}^2$ . His results are generally consistent with the results presented here.

The existence of a 4-day periodicity has been reported also in regard to oceanographic variables whose response appears forced by atmospheric variation. Thus, Groves [4] observed a 4-day spectral peak in time series of records of sea level in equatorial regions of the Pacific Ocean, correlated with similar fluctuation in wind speed data. Christensen and Rodriguez [5] note a 5 to 7-day oscillation in ocean currents, supposedly driven by atmospheric variation, off the coast of Baja, California. Similarly, Wunsch and Wimbush [6], and Düing, Mooers, and Lee [7] identify a broad spectral peak with periods from 4 to 7 days in current fluctuations off the Florida coast, correlated with atmospheric variability.

Two principal conclusions are drawn from the present analysis of wind speed data from the two stations in the Norwegian and Barents Seas, as well as from earlier studies of wind speed fluctuation.

1. Wind speed values considered over a sufficiently long time period follow a probability distribution that can be modeled, at least to a first level of approximation, as a Rayleigh distribution.

2. Wind speed fluctuations contain strong components at frequencies of one cycle per year and its harmonics. Most of the fluctuation power, however, occurs in a fairly broad spectral band with periods between 2 and 10 days. Because of this large spectral concentration of fluctuation power at from 2 to 10-day periods, it follows that ocean acoustic experiments whose purpose is to characterize seasonal variability of weather related phenomena, such as ambient noise, should be conducted over time periods sufficiently long to allow averaging over these synoptic variations.

## REFERENCES

1. C. R. C. *Standard Mathematical Tables*, Chemical Rubber Publishing Co. 12th ed. p. 391.
2. A. G. Davenport, "The Spectrum of Horizontal Gustiness Near the Ground in High Winds," *Quart. J. of the Royal Meteorological Society* 87, 194-211 (1961).
3. I. Van der Hoven, "Power Spectrum of Horizontal Wind Speed in the Frequency Range from 0.0007 to 900 Cycles per Hour," *J. Meteorology* 14, 160-164 (1957).
4. G. W. Groves, "Periodic Variation of Sea Level Induced by Equatorial Waves in the Easterlies," *Deep Sea Research* 3, 248-252 (1956).

ELLER AND BLODGETT

5. N. Christensen, Jr., and N. Rodriguez, "A Study of Sea Level Variations and Currents off Baja California," *J. Phys. Oceanography* 9, 631-638 (1979).
6. C. Wunsch and M. Wimbush, "Simultaneous Pressure, Velocity, and Temperature Measurements in the Florida Straits," *J. Marine Res.* 35, 75-104 (1977).
7. W. O. Düing, C. N. K. Mooers, and T. N. Lee, "Low-Frequency Variability in the Florida Current and Relations to Atmospheric Forcing from 1972 to 1974," *J. Marine Res.* 35, 129-161 (1977).



## Appendix

### FOURIER ANALYSIS OF WIND SPEED DATA

The wind speed can be expressed as a Fourier Series

$$W_k = A_o + \sum_{n=1}^N A_n \cos 2 \pi n \frac{t}{T_o} + \sum_{n=1}^N B_n \sin 2 \pi n \frac{t}{T_o},$$

where,

$T_o$  is the basic period of the data, and  
 $N$  is the highest term in the Fourier Series.

In this case the data were taken at 12-h intervals over a period of 2 yr giving  $T_o = 2 \text{ yr} = 1462 \times 12 \text{ h}$  and  $N = 1462/2 = 731$ .

Furthermore, time  $t$  changes in discrete steps, so  $t$  can be replaced by

$$t = kt_o, \quad (t_o = 12 \text{ h})$$

giving

$$W_k = A_o + \sum_{n=1}^N A_n \cos 2 \pi nk/1462 + \sum_{n=1}^N B_n \sin 2 \pi nk/1462.$$

By multiplying both sides of this equation by either  $\sin (2 \pi nk/1462)$  or  $\cos (2 \pi nk/1462)$ , summing over  $k$  from 1 to 1462, and using orthogonality rules, one finds

$$A_n = \frac{1}{731} \sum_{k=1}^{1462} W_k \cos \frac{2 \pi nk}{1462}, \text{ and}$$

$$B_n = \frac{1}{731} \sum_{k=1}^{1462} W_k \sin \frac{2 \pi nk}{1462}.$$

$A_o$  is, of course, the average of  $W_k$ .

The calling sequence for the Fourier transform subroutine is

CALL ANBN (W,K,A,B,C,N),

## ELLER AND BLODGETT

where

- $W$  = a Real \*4 array containing the time series  $W_k$ ,
- $K$  = an Integer \*4 variable defining the number of data points in the time series  $W_k$ ,
- $A$  = a Real \*4 array containing the  $A_n$  output elements of the transformation. The length of the array is  $N$ ,
- $B$  = A Real \*4 array containing the  $B_n$  output elements of the transformation. The length of the array is  $N$ ,
- $C$  = a Real \*4 array containing the  $\sqrt{A_n^2 + B_n^2}$  for each  $n$ . The length of the array is  $N$ , and
- $N$  = an Integer \*4 variable defining the total number of terms in the Fourier Series.

The total length of the subroutine is 00009300. It is compiled at the  $K$  level of the  $NX$  compiler. The program calculates values of the sin and cos using their recursive feature to compute the  $N$  terms in the Fourier Series. This speeds up the calculation. For this case where  $K = 1462$  and  $N = 731$  the total central processor time was 3.996 s. The program uses the following external routines: COS, SIN, DOTPRD, SQRT and FLOAT.

NRL REPORT 8436

```

0001      SUBROUTINE ANBN(W,K,A,B,C,N)
0002      DIMENSION W(K/2000/),A(N/1000/),B(N/1000/),C(N/1000/),
0003      1VCSS(2000),VSNN(2000),VC(2000),VS(2000)
0004      PHASE=(2.*3.14159265)/FLOAT(K)
0005      CON=1.0/FLOAT(N)
0006      DO 5 L=1,K
0007      VCSS(L)=COS(PHASE*L)
0008      VSNN(L)=SIN(PHASE*L)
0009      DO 7 I=1,N
0010      IBEG=I
0011      INC=I
0012      J=0
0013      10 CONTINUE
0014      DO 9 M=IBEG,K,INC
0015      J=J+1
0016      MTOP=M
0017      VC(J)=VCSS(M)
0018      VS(J)=VSNN(M)
0019      IF(J.EQ.K) GO TO 11
0020      IBEG=(MTOP+INC)-K
0021      GO TO 10
0022      11 A(I)=CON*DOTPRD(W,VC)
0023      B(I)=CON*DOTPRD(W,VS)
0024      CSQ=A(I)*A(I)+B(I)*B(I)
0025      C(I)=SQRT(CSQ)
0026      7 CONTINUE
0027      RETURN
0028      END

```